APEM journal
Advances in Production Engineering & Management
Volume 8 | Number 3 | September 2013 | pp 169–176
http://dx.doi.org/10.14743/apem2013.3.164
ISSN 1854-6250
Journal home: apem-journal.org

Synthesis of functionally graded material H13/Cu by LENS technology

Articek, U.[a,*], **Milfelner, M.**[a], **Anzel, I.**[b]

[a]EMO – Orodjarna d.o.o., Bezigrajska cesta 10, 3000 Celje, Slovenia, EU
[b]Faculty of Mechanical Engineering, University of Maribor, Smetanova ulica 17, 2000 Maribor, Slovenia, EU

ABSTRACT

Functionally Graded Material (FGM) is classified as advanced material characterized by variation in properties as the dimension varies. The overall properties of FGM are unique and different from any of the individual materials that form it. There is a wide range of applications for FGM. The tool and die industry is interested in depositing a material of high thermal conductivity onto steel in order to improve thermal management and productivity. Most dies in the casting industry for injection moulding are machined from premium grade H13 tool steel. These dies provide excellent performance in terms of mechanical properties and service life, however they are characterised by relatively low thermal conductivity. In this paper, we present an innovative use of the Laser Engineered Net Shaping (LENS) technology. We have explored the possibility of synthesis of FGM using tool steel H13 and copper. Results show successful fabrication of samples with LENS technology and represent a good potential for further development and use.

ARTICLE INFO

Keywords:
Laser cladding
Functionally graded material
Microstructural development
Mechanical properties

**Corresponding author:*
uros.articek@gmail.com
(Articek, U.)

Article history:
Received 15 February 2013
Revised 2 September 2013
Accepted 6 September 2013

1. Introduction

Functionally graded materials occur in nature as bones, teeth, bamboo etc., nature designed this materials to meet their expected service requirements. This idea is emulated from nature to solve engineering problems. FGM are a class of advanced materials of which the composition and microstructure change gradually from one side to the other, resulting in a corresponding variation in the properties. FGM have found their place in fields like medicine, automotive and aerospace, sport, electronics, optics, and nuclear applications, reactor components and energy conversion etc. [1]. Today, FGM can be divided into two broad groups, i.e. thin and bulk FGM. Thin FGM are relatively thin sections or thin surface coatings, while the bulk FGM are volume of materials which require more labour intensive processes. Thin section or surface coating FGM are produced by vapour deposition technique; Physical or Chemical Vapour Deposition (PVD/CVD), plasma spraying, electrodeposition, electrophoretic, Ion Beam Assisted Deposition (IBAD), Self-propagating High-temperature Synthesis (SHS) etc. Bulk FGM is produced using powder metallurgy technique, centrifugal casting method, solid freeform technology etc. [2].

In the injection moulding industry, new materials and technologies are required for mould dies in order to optimize production and keep costs as low as possible. Despite their excellent mechanical properties, tool steels that are nowadays used as materials for moulds limit productivity due to their low thermal conductivity. To solve this problem, designers are focusing on how to design the tool geometry and construction to achieve higher cooling rates. Complex cool-

ing channels are being designed to enable the cooling liquid to extract heat from the mould. Ejector pins, slides and air stream gates are used to eject the part from the mould cavity so the space left in it is small. An alternative way to solve this problem is the use of copper-beryllium inserts [3], which have higher thermal conductivity. However, they can leave marks on the part and are not environmentally friendly.

Therefore, new technologies and materials like Cu-deposition on tool steel or functionally graded materials with combination of high strength, wear resistance and thermal conductivity are explored as potential candidates for a more efficient injection moulding tool. Use of Direct Metal Deposition (DMD) fabrication process enables us to create an optimum configuration of fin trees and cooling channels as well as to use FGM without being concerned with the limitations of traditional manufacturing method [4, 5].

Many numerical methods [6], such as the Finite Element Method (FE), Finite Difference Method (FD), Boundary Value Problem (BV), Discrete Element Method (DEM), Material Point Method (MPM) etc., have been developed to investigate the thermal-mechanical performance [7], simulate the fatigue crack growth [8], determine the appropriate compositional gradient [9], analyse the distribution of thermal residual stresses [1] etc. of FGM. Each method has its advantages and limitations with regard to particular problems. The main challenge with the implementation of different methods in FGM analysis is to describe the material properties. At the moment, a large number of simulation software packages, like Abaqus, Ansys, Adina, COMSOL etc., is used. The use of classical finite elements for modelling the FGM structures is very difficult. To capture the variation of material properties, the finite element mesh has to be very fine, whereas each finite element has different constant material properties. Therefore, the need exists to improve existing numerical methods and develop new numerical methods for a numerical analysis of such materials. While studies on optimization are important for the development of future materials, technological limitations may undercut the applicability of some of the conclusions from these studies.

Laser Engineered Net Shaping™ (LENS) process is seen as one of the most promising DMD technologies for the production of such materials [10-12]. LENS is a relatively new technology that is capable of rapidly producing complex, fully dense parts directly from a Computer Aided Design (CAD). Deposition of material is done with a special laser head which is shown in Fig. 1. In the laser head is a lens which focuses the laser beam on the surface where it creates a small molten pool. In the molten pool powder is blown with the help of carrier gas. Some of the powder bounces of the surface and some is caught by the molten pool. The powder melts quickly when entering the molten pool and solidifies when the laser head moves away. The solidification is very quick because the heat is rapidly conducted away from the melt pool. The material is deposited in a shape of a line, which dimensions are set by the process parameters. Some of the important process parameters are laser power, powder flow rate, layer thickness, hatch width, deposition speed and oxygen level. One layer is made of a number of lines of deposited material. When one layer is finished, the laser head moves up for one layer thickness and begins building the next layer.

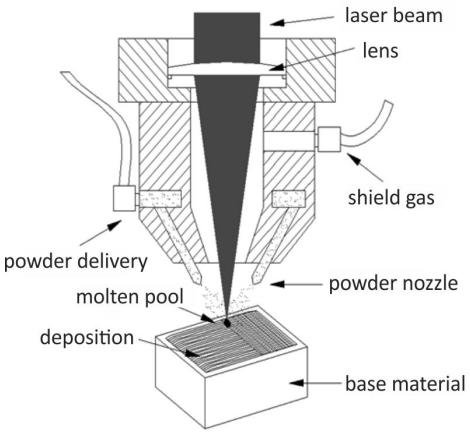

Fig. 1 Material deposition head

Table 1 Chemical composition of AISI H13 tool steel [15]

Element	Fe	Cr	Mo	Si	V	Mn	C	Ni
Composition (wt %)	balance	4.75-5.5	1.1-1.75	0.8-1.2	0.8-1.2	0.2-0.5	0.32-0.45	0.3 max

This procedure continues until the whole part is completed. Because the material in the process is melted, oxidation must be prevented. That is why the fabrication takes place under a controlled, inert atmosphere of argon.

The iron-copper (Fe-Cu) alloying system is one of the most suitable systems to produce an efficient FGM mould material [13]. Thermal conductivity of copper is approximately 13 times that of tool steel H13 (Table 1) at operating temperatures between 220-600 °C. Unfortunately, large solidification temperature range and high amount of Cu-rich terminal liquid over wide range of Cu concentration promote solidification cracking in Fe-Cu alloys [14]. Additionally, Fe-Cu phase diagram contains two peritectics and nearly flat liquidus; they exhibit a high tendency for non-equilibrium solidification that probably has a significant influence on susceptibility to cracking. At the same time, LENS is considered to be a technology that involves high velocity of solidification with a possibility of specific reactions, new phases and metastable microstructure formation. Moreover, the thermal impact of the solidifying layers on the microstructure of previously solidified layers and irregularities of previous layers is not known. While the properties of materials mainly depend on microstructure, it is important to know the microstructure development in the LENS process.

Our main objective was to explore the microstructure evolution of the LENS technology by FGM synthesis. As it is evident from the previous research, some chemical compositions are more susceptible to the formation of cracks by using DMD in Fe-Cu system [14]. We wanted to determine how the LENS technology influences the formation of cracks.

This paper presents recent results on the microstructure evolution and texture development and resulting mechanical properties of FGM samples produced by the LENS process.

2. Experimental work

Differences in material properties cause residual stresses. Many materials have a very small processing window. The first part of this work was to determine appropriate process parameters in order to achieve fully dense and defect-free samples. We produced a number of test samples with different mixtures of tool steel H13 and copper (H13-X wt % Cu; X = 25, 37.5, 50, 62.5, 75, 87.5). By analysing the process parameters and the obtained microstructures and mechanical properties of individual samples with fixed composition, we determined optimal parameter values used for the fabrication of FGM samples.

LENS 850-R machine made by Optomec Inc. was used with high power Nd:YAG laser with a capacity of 1000 W. We produced several cylindrical-shaped FGM samples (D = 10 mm, l = 100 mm) using the following parameters: laser power 440 W, traverse speed 6.2 mm/s, layer thickness 0.3 mm, hatch spacing 0.4 mm and hatch angle 60°, which were all held constant. The machine has a dual powder feeder system that allows simultaneous delivery of two different material mixtures. Powder particle size of H13 and copper ranged from 0.045 mm to 0.16 mm (Fig. 2). Powder was delivered by argon carrier gas (2 l/min) to the focus of the laser beam and was manufactured by gas atomisation; we selected the spherical shape which provides the solution to the porosity problem [16, 17]. The oxygen level was maintained under 10 ppm.

To evaluate the influence of microstructure on mechanical properties, tensile test and microhardness measurements were carried out. We compared the microstructure and mechanical properties of the LENS technology with conventional manufacturing technology of casting. We produced samples with the same chemical compositions as the LENS samples. The samples were made using mould casting technology. We used Vacuum Induction Melting (VIM) for casting H13 tool steel (Table 1) and Oxygen-Free High thermal Conductivity (OFHC) copper (99.99 % Cu) in argon inert gas. The moulds were cylindrical-shaped (D = 50 mm), machined from grey iron and had zirconium-oxide (ZrO_2) thin film as protective layer. The moulds were preheated to 400 °C

and provided with thermocouple type K (NiCr-Ni) temperature sensors. The solidification rate was relatively slow; the process was approximated to equilibrium solidification.

The static tensile testing using tensile device Zwick/Roell ZO 10 with a load cell capacity of 10 kN was performed for determining the mechanical properties. Measurements of mechanical properties were performed with tensile bars. With LENS technology, tensile bars were machined in the longitudinal orientation so that the axis was parallel to the cladding direction. The research conditions as well as the shapes and dimensions of the tensile test bars complied with the SIST EN 10002-1 standard. Tests were performed under constant speed of increasing deformation ν = 1.5 mm/min.

Measurements of hardness were carried out according to 6507-1:1998 standard by means of the Vickers test on the Zwick 3212 microhardness measurement device. For every sample, we performed 8 measurements.

The samples for optical and electron microscopy were cut out from the unstrained grip ends of the tensile bars. Samples were mounted, polished and etched according to standard metallographic procedures. Samples were polished to a 0.05 μm finish using Al_2O_3 suspension and etched with a solution (5 g $FeCl_3$, 10 ml HCl and 100 ml ethanol) for about 20 s. Scanning electron microscopy (SEM) was conducted at an accelerating voltage of 15 kV or 20 kV. After observation by optical microscopy (Nikon Epiphot 300) and scanning electron microscopy SEM (FEG Sirion 400 NC), some areas were chemically characterized by energy dispersion X-ray spectrometer EDX (INCA 6650).

Differential Scanning Calorimetry (DSC) was performed using a Netzsch STA 449F1 apparatus in order to determine the transformation temperatures and to identify the eventual occurrence of liquid separation as a consequence of metastable miscibility gap in Fe-Cu phase system. The samples for DSC analysis were formed into disks with a diameter of 6 mm and a high of 1 mm. The DSC analysis was performed in argon atmosphere with constant heating rate of 20 K/min and different cooling rates in the range from 2-45 K/min to reach different undercoolings, which is critical for liquid metastable phase separation. The melting points of Cu and pure Fe were used to calibrate the temperature scale of the facility to an accuracy of ± 1.5 K.

X-ray diffraction (XRD) was made on the surface of the treated samples by using Philips PW 1050 powder diffractometer with Ni filtered CuKα radiation (λ = 1.5418 Å) and scintillation detector within 2θ in the range 25-85°, in steps of 0.05°, with the scanning time of 3 s per step.

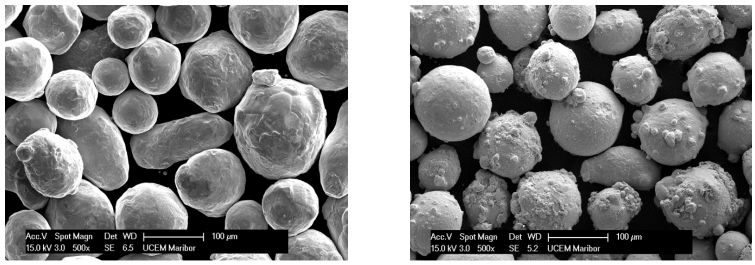

Fig. 2 SEM images of powders: Cu (left) and H13 tool steel (right)

3. Results and discussion

3.1 Microstructure of LENS samples

According to the Cu-Fe phase diagram [18], when an alloy is undercooled to a temperature inside the metastable miscibility gap, the homogeneous liquid may separate into two liquids: one is Cu-rich and the other is Fe-rich, Fig. 3. There are two different types of phase transformation mechanisms for liquid phase separation depending on the undercooling as well as the composition: nucleation and growth, and spinodal decomposition. At intermediate undercooling, when the melt enters the bimodal gap, nucleation and growth takes place, resulting in the formation of the spherical particles embedded in the matrix; whereas spinodal decomposition takes place, leading to the formation of the randomly interconnected network when the melt enters the spi-

nodal gap (large undercooling). In addition, at high cooling rates (about 10^3 °C/s), the crystallization kinetics are expected to be rapid enough to freeze the original morphology, i.e. the random network of the phase-separated melt. The solubility of Cu in Fe-rich phase and Fe in Cu-rich phase significantly exceeds the maximum solubility due to non-equilibrium rapid solidification. Generally, as the cooling rate becomes higher, the solidification becomes shorter, the undercooling becomes larger, and the microstructure becomes finer. The composition of the undercooled melt is another important factor that affects the occurrence of spinodal decomposition [19].

However, in our case, the phase-separated phases have different crystal structures, i.e. Fe-phase BCC (α_{Fe}) and Cu-phase FCC (γ_{Cu}). Therefore, rather than in the solid state, the spinodal decomposition took place in the undercooled melt before crystallization.

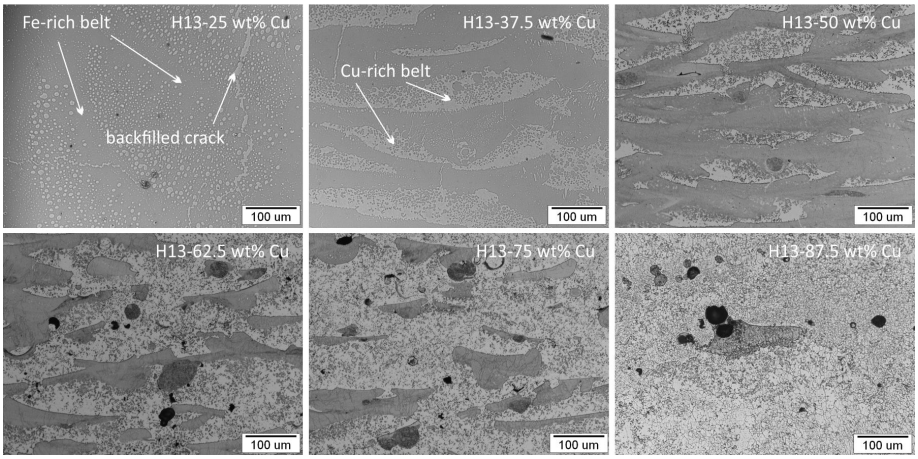

Fig. 3 Crack-free microstructures of individual LENS samples with fixed composition exhibit a randomly interconnected two-phase network structure (Cu-rich bright and Fe-rich dark regions)

Fig. 3 displays the different compositions of tool steel H13 and copper (H13-X wt % Cu ; X = 25, 37.5, 50, 62.5, 75, 87.5) produced by LENS technology that are not subject to solidification cracking despite the large solidification temperature range. An important factor is the amount of terminal liquid available for the backfilling of cracks that may form during solidification. The terminal liquid is defined as the volume of liquid present at the end of solidification. This terminal liquid transforms to the Cu-rich phase at the end of solidification. Terminal reaction during non-equilibrium solidification is almost pure Cu. The amount of terminal liquid can be determined by measuring the amount of Cu in the deposits.

3.2 Microstructure of FGM samples

The direct interface between two distinctive materials can cause stress. The FGM theory implies that the stress can be minimized when gradual transitions between these two materials exist. FGM may be characterized by the variation in composition and structure gradually over volume, resulting in corresponding changes in material properties. These transitions can be found in two ways: continuous or discrete.

In our case, the composition of FGM by the LENS technology exhibits stepped changes (discrete), however the composition in the melt boundary area changes due to dilution and thermal impact of the next layer in the way for a layer to become enriched with the newly clad layer. Partially mixed zones occur continuously and are generally very small in relation to the deposit size. In this way, near linear changes in chemical composition are achieved. FGM samples were clad on base material, whereby the chemical composition changed by 10 wt % for every 10 layers, Fig. 4.

The composition of each FGM layer, depends on the degree of dilution between the substrate (previous layer) and powder material. The dilution varies with changes in powder feed rate, laser power, and traverse speed. Microstructure characterisations indicate good metallurgical bonding of individual layers of LENS deposits.

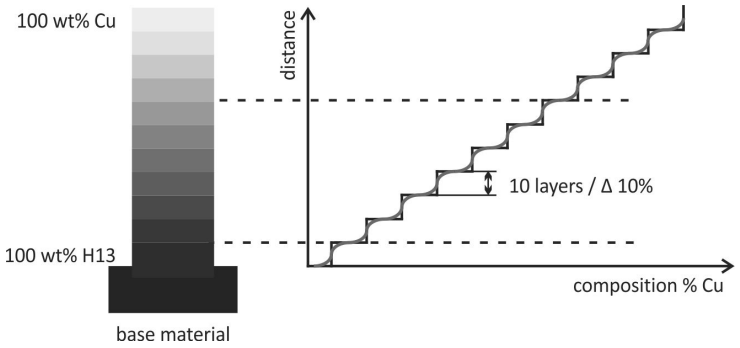

Fig. 4 Schematic illustration of continuously graded material H13-Cu

The main goal of this research was to evaluate the cracking susceptibility of continuously graded deposit from pure H13 to pure Cu. As is evident from the previous research [14], cracking was observed in deposits with Cu concentration between approximately 5 and 43 wt %. Our FGM microstructure shows Fig. 5 that this composition range does not include solidification cracking because it is believed that enough amount of terminal Cu-rich phase was presented at the end of solidification for backfilling all cracks that may form.

As it is evident from the Fig. 5, cracks are negligible and only noticeable in the composition range around 10 wt % Cu as they are present in small quantities and are short in length. As H13 is a high carbon content steel, the carbon also contributed to martensite formation, which is fragile and has low ductility causing cracks. These cracks could have been eliminated by optimising process parameters for that composition. As we used constant parameters for the whole FGM composition range, we did not consider that composition when analysing the process parameters for FGM. By optimising the process parameters for every 10 wt % of composition, we could have achieved crack-free microstructure even around composition range of 10 wt % Cu. This will be considered in our further research.

In the aforementioned research, powder was also not optimized for the process. The copper powder morphology was dendritic, which resulted in gas being trapped in the melt pool as it rapidly solidified. In our case, the spherical powder solves this defect to a large extent, however, uniformly distributed micro-spherical type gas porosity was still partially present. Photomicrograph (Fig. 5) clearly shows the presence of porosity, indicated by small dark spots. Porosity occurs when bubbles of gas (argon) are trapped in the bead after solidification.

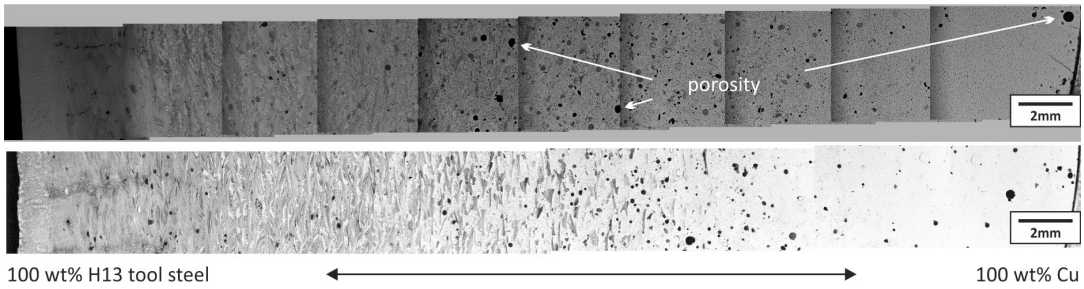

Fig. 5 Evaluation of the FGM H13-Cu microstructure. A small amount of gas pores is present.

3.3 Mechanical properties

The solidification parameters and chemical composition of alloys directly affect the microstructure of the alloy systems, and also significantly influence their mechanical behaviours (Fig. 6). LENS samples have higher tensile strength values than cast samples, whereas cast samples are more ductile. This is due to their microstructure, which is finer and more homogenous in LENS samples because solidification occurs at higher rates. Elongation (ε) of cast samples is greater than the elongation of LENS samples. This is due to different solidification rates of alloys.

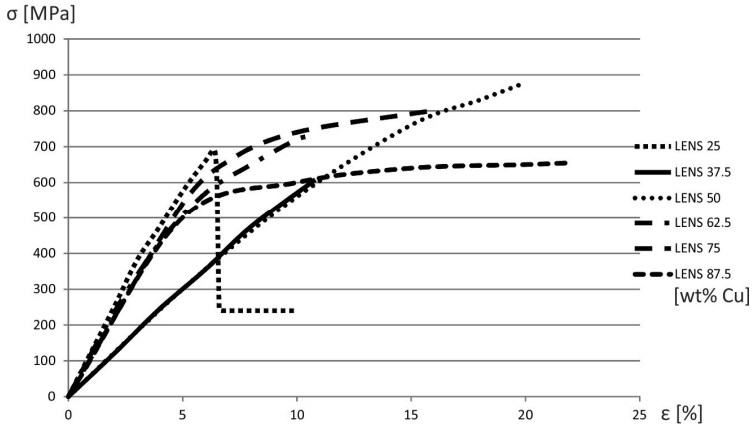

Fig. 6 Stress-strain curves of LENS H13-X wt % Cu (X = 25, 37.5, 50, 62.5, 75, 87.5) alloys at room temperature

LENS microstructure is the result of faster cooling and solidification – metastable solidification where matrix with higher strength forms (containing more alloying elements and precipitates due to which ε is smaller). There is a trend of LENS samples having a slightly higher value of elastic modulus E than cast samples because they are more metastable due to a greater number of alloying elements, which affects the bond strength.

The characteristics of microstructure are reflected in the results of microhardness measurements. Very fine-grained microstructure, smaller size and larger quantity of uniformly distributed spherical phase and the content of alloying elements in matrix result in significantly higher average microhardness values of LENS samples. Table 2 shows the average measures of microhardness values of the LENS and cast samples at different positions on samples. Each specimen was measured randomly eight times for the average value.

Table 2 Vickers microhardness results were recorded as the average values of measurements

	25 wt % Cu	37.5 wt % Cu	50 wt % Cu	62.5 wt % Cu	75 wt % Cu	87.5 wt % Cu
LENS	594 HV	525 HV	469 HV	527 HV	502 HV	305 HV
CASTING	458 HV	221 HV	334 HV	449 HV	207 HV	118 HV

4. Conclusion

It has been shown that it is technically feasible to apply crack-free functionally graded materials by LENS technology. Graded layers were built up with a smooth transition of composition, and only low and uniformly distributed porosity was present. This is due to gas atomisation of spherical-shape powders and optimized process parameters.

The mechanical properties of the LENS samples are superior in comparison to the conventional casted samples. The tensile data and microstructure characterisation indicate good metallurgical bonding of individual layers of LENS deposits.

It has been shown that FGM H13-Cu alloy fabricated with LENS technology can perform well in real-life applications. Good thermal conductivity of copper and high wear resistance of steel can be achieved without cracks as well as better mechanical properties. Moulds produced with the LENS technology can have distinctive regions with higher heat conduction. Higher rates of heat transfer from thicker regions of the injected part can be useful for the production of better and cheaper injection moulded polymer parts. The application area of the tool and die industry can be further enhanced and extended by bringing down the fabrication costs, as well as by improving thermal management and productivity.

There are many other areas that still need to be tackled in order to produce complex FGM materials. Future work will involve the determination of the best laser processing parameters for each blend according to the chemical composition to achieve a proper cooling rate for crack-free fabrication and good mechanical properties. It is necessary to determine compatible compositions for a rapid transition to the desired concentration of an individual alloy element to achieve optimum mechanical and physical properties.

Acknowledgement

The Research is partially funded by the European Social Fund. Invitations to tenders for the selection of the operations are carried out under the Operational Programme for Human Resources Development for 2007-2013, 1. development priority: Promoting entrepreneurship and adaptability, the priority guidelines 1.1: Experts and researchers for enterprises to remain competitive.

References

[1] Arash, H.D. (2012). *Finite element analysis of thermally induced residual stresses in functionally graded materials*, PhD Thesis, KTH, School of Industrial Engineering and Management (ITM), Materials Science and Engineering, Stockholm, Sweden.
[2] Mahamood, R.M., Akinlabi, E.T., Shukla, M., Pityana, S. (2012). Functionally graded material: an overview, In: *Proceedings of the World Congress on Engineering, Vol. III*, 1593-1597, London.
[3] Rebelo, J.C., Dias, A.M., Mesquita, R., Vassalo, P., Santos, M. (2000). An experimental study on electro-discharge machining and polishing of high strength copper-beryllium alloys, *Journal of Materials Processing Technology*, Vol. 103, No. 3, 389-397, doi: 10.1016/S0924-0136(99)00492-6.
[4] Beal, V.E., Erasenthiran, P., Hopkinson, N., Dickens, P., Ahrens, C.H. (2006). Optimisation of processing parameters in laser fused H13/Cu materials using response surface method (RSM), *Journal of Materials Processing Technology,* Vol. 174, No. 1-3, 145-154, doi: 10.1016/j.jmatprotec.2005.04.101.
[5] Jiang, W., Nair, R., Molian, P. (2005). Functionally graded mold inserts by laser-based flexible fabrication: processing modeling, structural analysis, and performance evaluation, *Journal of Materials Processing Technology*, Vol. 166, No. 2, 286-293, doi: 10.1016/j.jmatprotec.2004.08.029.
[6] Birman, V., Byrd, L.W. (2007). Modeling and analysis of functionally graded materials and structures, *Applied Mechanics Reviews,* Vol. 60, No. 5, 195-216, doi: 10.1115/1.2777164.
[7] Saifullah, A.B.M., Masood, S.H., Sbarski, I. (2012). Thermal-structural analysis of bi-metallic conformal cooling for injection moulds, *The International Journal of Advanced Manufacturing Technology*, Vol. 62, No. 1-4, 123-133, doi: 10.1007/s00170-011-3805-5.
[8] Bhattacharya, S., Singh, I.V., Mishra, B.K. (2013). Mixed-mode fatigue crack growth analysis of functionally graded materials by XFEM, *International Journal of Fracture*, Vol. 183, No. 1, 81-97, doi: 10.1007/s10704-013-9877-5.
[9] Cadman, J.E., Zhou, S., Chen, Y., Li, Q. (2013). On design of multi-functional microstructural materials, *Journal of Materials Science*, Vol. 48, No. 1, 51-66, doi: 10.1007/s10853-012-6643-4.
[10] Zheng, B., Zhou, Y., Smugeresky, J.E., Schoenung, J.M., Lavernia, E.J. (2008). Thermal behavior and microstructural evolution during laser deposition with Laser-Engineered Net Shaping: Part I. Numerical Calculations, *Metallurgical and Materials Transactions*, Vol. 39A, 2228-2236, doi: 10.1007/s11661-008-9557-7.
[11] Dong-Gyu, A., (2011). Applications of laser assisted metal rapid tooling process to manufacture of molding & foming tools – state of the art, *International Journal of Precision Engineering and Manufacturing*, Vol. 12, No. 5, 925-938, doi: 10.1007/s12541-011-0125-5.
[12] Imran, M.K., Masood, S.H., Brandt, M., Bhattacharya, S., Mazumder, J. (2011). Direct metal deposition (DMD) of H13 tool steel on copper alloy substrate: Evaluation of mechanical properties, *Materials Science and Engineering*, Vol. 528, No. 9, 3342-3349, doi: 10.1016/j.msea.2010.12.099.
[13] Beal, V.E., Erasenthiran, P., Hopkinson, N., Dickens, P., Ahrens, C.H. (2006). The effect of scanning strategy on laser fusion of functionally graded H13/Cu materials, *The International Journal of Advanced Manufacturing Technology*, Vol. 30, 844-852, doi: 10.1007/s00170-005-0130-x.
[14] Noecker II, F.F., DuPont, J.N. (2007). Microstructural development and solidification cracking susceptibility of Cu deposits on steel: Part I, *Journal of Materials Science*, Vol. 42, No. 2, 495-509, doi: 10.1007/s10853-006-1258-2.
[15] ASM Metals Handbook (2005). *Properties and selection: iron, steels, and high performance alloys*, Vol. 1, ASM International Handbook Committee.
[16] Susan, D.F., Puskar, J.D., Brooks, J.A., Robino, C.V. (2006). Quantitative characterization of porosity in stainless steel LENS powders and deposits, *Materials Characterization*, Vol. 57, No. 1, 36-43, doi: 10.1016/j.matchar. 2005.12.005.
[17] Pinkerton, A.J., Li, L. (2005). Direct additive laser manufacturing using gas- and water-atomised H13 tool steel powders, *The International Journal of Advanced Manufacturing Technology*, Vol. 25, No. 5-6, 471-479, doi: 10.1007/s00170-003-1844-2.
[18] Swartzendruber, L.J. (1990). *Binary Alloy Phase Diagrams*, 2nd ed., Massalski, T.B. (ed.), ASM, New York, 1408-1409.
[19] Wilde, G., Willnecker, R., Singh, R.N., Sommer, F. (1997). The metastable miscibility gap in the system Fe-Cu, *Zeitschrift für Metallkunde*, Vol. 88, No. 10, 804-809.